

# Extension of Dirac equation by the charge creation-annihilation field model and simulation for formation process of atomic orbitals by FDTD method

Hideki Mutoh\*

*Link Research Corporation, Odawara, Kanagawa 250-0055, Japan*

(Dated: June 30, 2022)

We have reported that Maxwell's equations should be extended by using the charge creation-annihilation field to treat the charge generation-recombination in semiconductor devices. Considering the charge creation-annihilation field, the extended Maxwell's and Dirac equations can be given by the same formula consisting of the dual 4-vector fields and the 8 by 8 spatially symmetric differential operator matrix. By using FDTD 3D simulations, we found that the Dirac field wave packet with enough smaller velocity than light can be stably created without explicit consideration of Zitterbewegung, although it is difficult in 1D simulations. We calculated the Dirac field propagation in the electric central force potential and succeeded to simulate the formation process of atomic orbitals based on the extended Dirac equation by this method without any physical approximation for the first time. A small unstable orbital appears at first and rapidly grows and finally becomes to a large stable orbital with the same radius as Bohr radius divided by the atomic number given by Schrödinger equation. This result could be regarded as a proof of correctness of the charge creation-annihilation field model.

KEYWORDS: charge creation-annihilation field, Dirac equation, Maxwell's equations, FDTD method, atomic orbital

## I. INTRODUCTION

In semiconductors, generation and recombination of charge pairs occur by light irradiation or thermal excitation. Since this phenomenon cannot be handled by Maxwell's equations, we have proposed to extend them by adding the charge creation-annihilation field, which is almost equivalent to Nakanishi-Lautrap field in quantum electrodynamics [1–3]. We found that the weak gravitational field can be given by the same formula as the extended Maxwell's equations and classical and quantum mechanics are derived from the equation by assuming that the gravitational wave is not generated or negligibly small by stable motion under the weak gravitational field. In this paper we show that Dirac equations can be also given by the same formula as the extended Maxwell's equations, which consists of the dual 4-vector fields and the 8 by 8 spatially symmetric differential operator matrix. Since Finite Difference Time Domain (FDTD) method [4] can be used for transient analysis of electromagnetic field, it could be used for that of Dirac field [5, 6]. We calculated the Dirac field propagation in electric field by FDTD method based on the extended Dirac equation, so that we obtained interesting results about stability of the Dirac field propagation and the formation process of atomic orbitals.

## II. EXTENSION OF DIRAC EQUATION

Dirac equation is given by

$$(i\hbar\gamma^\mu\partial_\mu - mc)\psi = 0, \quad (1)$$

where  $\hbar$  is Planck constant,  $\psi$  is a wave function vector consisting of four components,  $m$  is a mass,  $c$  is light speed in free space, and  $\gamma^\mu$  are gamma matrices which satisfy the following equation[7–10].

$$\frac{1}{2}(\gamma^\mu\gamma^\nu + \gamma^\nu\gamma^\mu) = \eta^{\mu\nu} \equiv \begin{cases} 1 : & \mu = \nu = 0 \\ 0 : & \mu \neq \nu \\ -1 : & \mu = \nu = 1, 2, 3 \end{cases}. \quad (2)$$

For example, gamma matrices are given by

$$\gamma^0 = \begin{pmatrix} 1 & 0 & 0 & 0 \\ 0 & 1 & 0 & 0 \\ 0 & 0 & -1 & 0 \\ 0 & 0 & 0 & -1 \end{pmatrix}, \gamma^1 = \begin{pmatrix} 0 & 0 & 0 & 1 \\ 0 & 0 & 1 & 0 \\ 0 & -1 & 0 & 0 \\ -1 & 0 & 0 & 0 \end{pmatrix},$$

$$\gamma^2 = \begin{pmatrix} 0 & 0 & 0 & -i \\ 0 & 0 & i & 0 \\ 0 & i & 0 & 0 \\ -i & 0 & 0 & 0 \end{pmatrix}, \gamma^3 = \begin{pmatrix} 0 & 0 & 1 & 0 \\ 0 & 0 & 0 & -1 \\ -1 & 0 & 0 & 0 \\ 0 & 1 & 0 & 0 \end{pmatrix}. \quad (3)$$

These matrices have spatial asymmetry, which means that only one or two of  $\gamma^1$ ,  $\gamma^2$ , and  $\gamma^3$  include imaginary numbers. Since it is difficult to calculate propagation of Dirac fields by FDTD method in the above case as shown later, Dirac equation should be extended to consist of spatially symmetric matrices as follows.

$$\left(\bar{\gamma}^\mu\partial_\mu + \frac{mc}{\hbar}\bar{\gamma}^4\right)\psi = 0, \quad (4)$$

---

\* hideki.mutoh@nifty.com

where  $\bar{\gamma}^1$ ,  $\bar{\gamma}^2$ , and  $\bar{\gamma}^3$  are real number matrices and  $\bar{\gamma}^\mu$  ( $\mu = 0, 1, 2, 3, 4$ ) satisfy

$$\frac{1}{2}(\bar{\gamma}^\mu \bar{\gamma}^\nu + \bar{\gamma}^\nu \bar{\gamma}^\mu) = \bar{\eta}^{\mu\nu} \equiv \begin{cases} 1 : & \mu = \nu = 0, 4 \\ 0 : & \mu \neq \nu \\ -1 : & \mu = \nu = 1, 2, 3 \end{cases}, \quad (5)$$

where  $\bar{\gamma}^\mu$  cannot be represented by  $4 \times 4$  matrices. Eqs. (4) and (5) give Klein-Gordon equation

$$\left( \bar{\gamma}^\mu \partial_\mu + \frac{mc}{\hbar} \bar{\gamma}^4 \right)^2 \psi = \left( \square + \frac{m^2 c^2}{\hbar^2} \right) \psi = 0, \quad (6)$$

where  $\square$  is d'Alembertian defined by  $\square \equiv \partial_0^2 - \nabla^2$ . In order to obtain  $\bar{\gamma}^\mu$ , we consider about extension of Maxwell's equations. The extended Maxwell's equations including charge creation-annihilation field are given by [11–16]

$$\begin{aligned} \mathbf{J} &= \frac{1}{\mu} \nabla \times \mathbf{B} - \epsilon \frac{\partial \mathbf{E}}{\partial t} + \frac{1}{\mu} \nabla N, \\ \rho &= \epsilon \nabla \cdot \mathbf{E} - \epsilon \frac{\partial N}{\partial t}, \\ 0 &= \nabla \times \mathbf{E} + \frac{\partial \mathbf{B}}{\partial t}, \\ 0 &= \nabla \cdot \mathbf{B}, \end{aligned} \quad (7)$$

where  $\mathbf{J}$  and  $\rho$  are current and charge density,  $\epsilon$  and  $\mu$  are permittivity and permeability,  $\mathbf{E}$ ,  $\mathbf{B}$ , and  $N$  are electric, magnetic, and the charge creation-annihilation fields, respectively. Eq. (7) directly gives the following equation of the charge conservation,

$$\nabla \mathbf{J} + \frac{\partial \rho}{\partial t} = -\frac{1}{\mu} \square N = G, \quad (8)$$

where  $G$  is the charge generation rate, which is an important parameter in semiconductor physics[17–19]. Here  $\mathbf{E}$ ,  $\mathbf{B}$ , and  $N$  satisfy

$$\begin{aligned} \mathbf{E} &= -\nabla \psi - \frac{\partial \mathbf{A}}{\partial t}, \\ \mathbf{B} &= \nabla \times \mathbf{A}, \\ \xi N &= -\nabla \cdot \mathbf{A} - \frac{\partial \psi}{c^2 \partial t}, \end{aligned} \quad (9)$$

where  $\mathbf{A}$  and  $\psi$  are vector and scalar potential and  $\xi$  is a gauge parameter. Then, Eqs. (7) and (9) can be written by using differential operator matrices as follows.

$$\mu \begin{pmatrix} ic\rho \\ J^1 \\ J^2 \\ J^3 \end{pmatrix} = \begin{pmatrix} i\partial_0 & \partial_1 & \partial_2 & \partial_3 \\ -\partial_1 & i\partial_0 & -\partial_3 & \partial_2 \\ -\partial_2 & \partial_3 & i\partial_0 & -\partial_1 \\ -\partial_3 & -\partial_2 & \partial_1 & i\partial_0 \end{pmatrix} \begin{pmatrix} -N \\ B^1 + iE^1/c \\ B^2 + iE^2/c \\ B^3 + iE^3/c \end{pmatrix}, \quad (10)$$

$$\begin{pmatrix} -\xi N \\ B^1 + iE^1/c \\ B^2 + iE^2/c \\ B^3 + iE^3/c \end{pmatrix} = \begin{pmatrix} -i\partial_0 & \partial_1 & \partial_2 & \partial_3 \\ -\partial_1 & -i\partial_0 & -\partial_3 & \partial_2 \\ -\partial_2 & \partial_3 & -i\partial_0 & -\partial_1 \\ -\partial_3 & -\partial_2 & \partial_1 & -i\partial_0 \end{pmatrix} \begin{pmatrix} i\psi/c \\ A^1 \\ A^2 \\ A^3 \end{pmatrix}. \quad (11)$$

Now we define four vectors  $J$ ,  $A$ ,  $F$ , and  $\bar{F}$  as follows.

$$\begin{aligned} J &\equiv \begin{pmatrix} ic\rho \\ \mathbf{J} \end{pmatrix}, \quad A \equiv \begin{pmatrix} i\psi/c \\ \mathbf{A} \end{pmatrix}, \\ F &\equiv \begin{pmatrix} -N \\ \mathbf{B} + i\mathbf{E}/c \end{pmatrix}, \quad \bar{F} \equiv \begin{pmatrix} -\xi N \\ \mathbf{B} + i\mathbf{E}/c \end{pmatrix}. \end{aligned} \quad (12)$$

We can obtain the following equations.

$$\begin{aligned} \mu J &= \delta^\mu \partial_\mu F, \\ \bar{F} &= \delta^{\mu*} \partial_\mu A, \end{aligned} \quad (13)$$

where  $\delta^\mu$  are the following spatially symmetric matrices.

$$\begin{aligned} \delta^0 &= \begin{pmatrix} i & 0 & 0 & 0 \\ 0 & i & 0 & 0 \\ 0 & 0 & i & 0 \\ 0 & 0 & 0 & i \end{pmatrix}, \quad \delta^1 = \begin{pmatrix} 0 & 1 & 0 & 0 \\ -1 & 0 & 0 & 0 \\ 0 & 0 & 0 & -1 \\ 0 & 0 & 1 & 0 \end{pmatrix}, \\ \delta^2 &= \begin{pmatrix} 0 & 0 & 1 & 0 \\ 0 & 0 & 0 & 1 \\ -1 & 0 & 0 & 0 \\ 0 & -1 & 0 & 0 \end{pmatrix}, \quad \delta^3 = \begin{pmatrix} 0 & 0 & 0 & 1 \\ 0 & 0 & -1 & 0 \\ 0 & 1 & 0 & 0 \\ -1 & 0 & 0 & 0 \end{pmatrix}. \end{aligned} \quad (14)$$

Eq. (13) can be written as follows.

$$\begin{pmatrix} \bar{F} \\ \mu J \end{pmatrix} = \begin{pmatrix} 0 & \delta^{\mu*} \partial_\mu \\ \delta^\mu \partial_\mu & 0 \end{pmatrix} \begin{pmatrix} F \\ A \end{pmatrix}. \quad (15)$$

We call Eqs. (7) - (15) the charge creation-annihilation field model. Now we define matrices  $\bar{\gamma}^\mu$  ( $\mu = 0, 1, 2, 3$ ) and  $\bar{\gamma}^4$  as

$$\bar{\gamma}^\mu \equiv \begin{pmatrix} 0 & \delta^{\mu*} \\ \delta^\mu & 0 \end{pmatrix}, \quad \bar{\gamma}^4 \equiv \begin{pmatrix} I_4 & 0 \\ 0 & -I_4 \end{pmatrix}, \quad (16)$$

where  $I_4$  is  $4 \times 4$  unit matrix. Since  $\bar{\gamma}^\mu$  ( $\mu = 0, 1, 2, 3, 4$ ) satisfy Eq. (5), we obtain the 8 elements extended Dirac equation of Eq. (4). When we introduce 4 elements wave functions  $\psi_A$  and  $\psi_B$  to satisfy

$$\psi = \begin{pmatrix} \psi_A \\ \psi_B \end{pmatrix}, \quad (17)$$

Eq. (4) is rewritten as

$$\begin{pmatrix} mc/\hbar & \delta^{\mu*} \partial_\mu \\ \delta^\mu \partial_\mu & -mc/\hbar \end{pmatrix} \begin{pmatrix} \psi_A \\ \psi_B \end{pmatrix} = 0. \quad (18)$$

Then we obtain

$$\begin{aligned} i\partial_0 \psi_A + \delta^k \partial_k \psi_A - \frac{mc}{\hbar} \psi_B &= 0, \\ -i\partial_0 \psi_B + \delta^k \partial_k \psi_B + \frac{mc}{\hbar} \psi_A &= 0. \end{aligned} \quad (19)$$

When  $\dagger$  means Hermite conjugate, we obtain

$$\begin{aligned} -i\partial_0 \psi_A^\dagger - \partial_k \psi_A^\dagger \delta^k - \frac{mc}{\hbar} \psi_B^\dagger &= 0, \\ i\partial_0 \psi_B^\dagger - \partial_k \psi_B^\dagger \delta^k + \frac{mc}{\hbar} \psi_A^\dagger &= 0. \end{aligned} \quad (20)$$

Here we define four current  $C^\mu$  as follows.

$$\begin{aligned} C^0 &\equiv \psi_A^\dagger \psi_A + \psi_B^\dagger \psi_B = \psi^\dagger \psi, \\ C^k &\equiv -i(\psi_A^\dagger \delta^k \psi_A - \psi_B^\dagger \delta^k \psi_B). \end{aligned} \quad (21)$$

Then Eqs. (19) - (21) give

$$\partial_\mu C^\mu = 0. \quad (22)$$

Now we define  $\bar{\psi}^\dagger$  as

$$\bar{\psi}^\dagger \equiv \psi^\dagger \bar{\gamma}^0. \quad (23)$$

Then we obtain

$$C^\mu = \bar{\psi}^\dagger \bar{\gamma}^\mu \psi. \quad (24)$$

Therefore,  $C^0$  and  $C^k$  can be regraded as probability density and probability current density, respectively.

Next we consider about spin. When we introduce  $\psi_+$  and  $\psi_-$  as

$$\begin{aligned} \psi_+ &\equiv \psi_A + \psi_B, \\ \psi_- &\equiv \psi_A - \psi_B, \end{aligned} \quad (25)$$

Eq. (19) is rewritten as

$$\begin{aligned} i\partial_0 \psi_+ + \delta^k \partial_k \psi_- - \frac{mc}{\hbar} \psi_+ &= 0, \\ i\partial_0 \psi_- + \delta^k \partial_k \psi_+ + \frac{mc}{\hbar} \psi_- &= 0. \end{aligned} \quad (26)$$

Under vector potential  $\mathbf{A}$  and scalar one  $\phi$ , we should substitute  $\partial_k + ieA_k/\hbar c$  for  $\partial_k$  and  $\partial_0 - ie\phi/\hbar c$  for  $\partial_0$  in the equations. When we assume that  $E$  is total energy and the time dependence of the wave functions is  $\exp(-iEt/\hbar)$ , we could substitute  $-iE/\hbar c$  for  $\partial_0$  as

$$\begin{aligned} \left( \frac{E}{\hbar c} + \frac{e}{\hbar c} \phi - \frac{mc}{\hbar} \right) \psi_+ + \partial^k \left( \partial_k + \frac{ie}{\hbar c} A_k \right) \psi_- &= 0, \\ \left( \frac{E}{\hbar c} + \frac{e}{\hbar c} \phi + \frac{mc}{\hbar} \right) \psi_- + \partial^k \left( \partial_k + \frac{ie}{\hbar c} A_k \right) \psi_+ &= 0. \end{aligned} \quad (27)$$

Considering nonrelativistic condition,

$$E = E_{NR} + mc^2, \quad (28)$$

where  $E_{NR}$  is nonrelativistic energy. When we assume  $|E_{NR}| \ll mc^2$  and  $|e\phi| \ll mc^2$ , Eq. (26) gives

$$\psi_- \approx -\frac{\hbar}{2mc} \delta^k \left( \partial_k + \frac{ie}{\hbar c} A_k \right) \psi_+. \quad (29)$$

Then Eqs. (27) and (29) give

$$\begin{aligned} (E_{NR} + e\phi) \psi_+ &= \frac{\hbar^2}{2m} \delta^k \left( \partial_k + \frac{ie}{\hbar c} A_k \right) \delta^k \left( \partial_k + \frac{ie}{\hbar c} A_k \right) \psi_+ \\ &= \left\{ -\frac{\hbar^2}{2m} \left( \nabla + \frac{ie}{\hbar c} \mathbf{A} \right)^2 + \frac{ie\hbar}{2mc} \delta^k B_k \right\} \psi_+. \end{aligned} \quad (30)$$

Therefore, the second term of right side of the above equation shows the magnetic moment  $-i\hbar/2mc$ . When we define  $s^k$  as

$$s^k \equiv -\frac{i\hbar}{2} \delta^k, \quad (31)$$

we obtain

$$\begin{aligned} s^1 s^2 - s^2 s^1 &= i\hbar s^3, \\ s^2 s^3 - s^3 s^2 &= i\hbar s^1, \\ s^3 s^1 - s^1 s^3 &= i\hbar s^2, \\ (s^1)^2 + (s^2)^2 + (s^3)^2 &= \frac{3}{4} \hbar^2. \end{aligned} \quad (32)$$

Therefore,  $s$  is a spin operator with spin quantum number of  $1/2$ . Eq. (30) can be regarded as the wave equation of a particle with spin quantum number of  $1/2$  under vector potential  $\mathbf{A}$  and scalar one  $\phi$ .

### III. DIRAC FIELD PROPAGATION ANALYSIS BY FDTD METHOD

Since Dirac equation is quite similar to Maxwell's equations, Dirac field propagation could be calculated by FDTD method, which is often used for propagation analysis of electromagnetic field. We compared the calculation result by FDTD method based on between conventional four vector and the extended eight vector Dirac equations. Figure 1 shows the analyzed structure consisting of a cube with a side length  $L$  of 10 pm, where the origin exists at the center of the cube. The Dirac field wave packet is created by vibration of the top surface of the structure. We adopt the following wave function as the initial wave packet of Dirac field, which has a finite value in the whole region and satisfies Klein-Gordon equation.

$$\psi = \frac{\sin(kr') \exp(-i\omega t')}{kr'}, \quad (33)$$

where  $r'$  and  $t'$  satisfy the following equations by using the wave packet moving velocity  $v$  and  $\beta \equiv v/c$ .

$$\begin{aligned} r' &= \sqrt{x^2 + y^2 + \frac{(z - vt')^2}{1 - \beta^2}}, \\ t' &= \frac{1}{\sqrt{1 - \beta^2}} \left( 1 - \frac{vz}{c^2} \right). \end{aligned} \quad (34)$$

$k$  and  $\omega$  are wave number and angular frequency, respectively, and satisfy

$$k^2 = \frac{\omega^2}{c^2} - \frac{m^2 c^2}{\hbar^2}. \quad (35)$$

Figure 2 shows the definition position of the elements for conventional and extended Dirac fields in FDTD method calculation. The position of the 4 elements conventional Dirac field is spatially asymmetric, while that

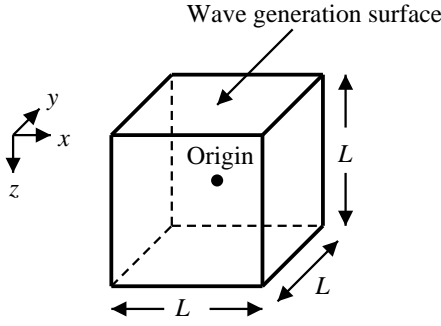


FIG. 1. Analyzed structure.

of the 8 elements extended Dirac field is spatially symmetric. Figure 3 and 4 show the wave packet shape dependence on the propagation time in the 4 and 8 elements cases, respectively. Figure 5 shows that the moving distance of the wave packet peak is equal to the product of the wave packet velocity and propagation time in the above cases, although 1-D like calculation gives the wave packet speed as same as the light speed in free space, where only  $\psi_1$  and  $\psi_3$  are solved. We found that explicit consideration of Zitterbewegung [20, 21] is unnecessary for 3-D analysis, although it is necessary for 1-D analysis. As shown in Fig. 6, we found that the wave packet peak intensity decreases with increase of propagation time in the 4 elements case, although it is almost constant except early period in the 8 elements case. The difference of stability between the 4 and 8 elements wave packets could be caused by the symmetry difference of definition position for the Dirac field elements as shown in Fig. 2.

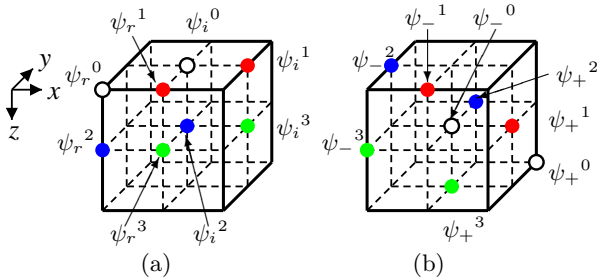


FIG. 2. Definition position for the Dirac field elements in the cell of FDTD method. a: conventional Dirac field, where  $\psi_r$  and  $\psi_i$  denote the real and imaginary parts, b: extended Dirac field, white:  $\psi^0$ , red:  $\psi^1$ , blue:  $\psi^2$ , green:  $\psi^3$ .

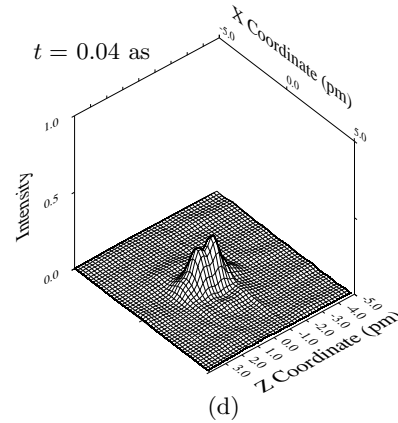
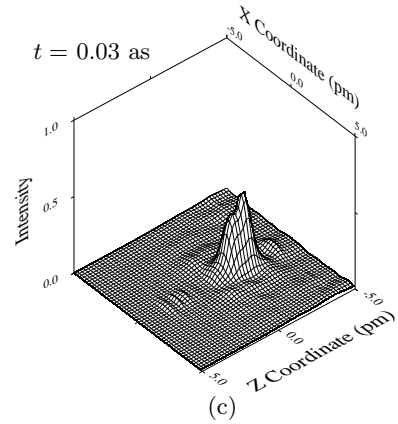
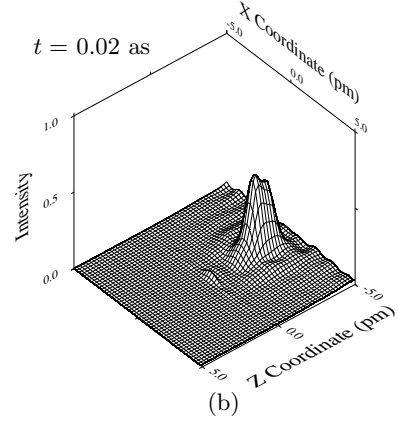
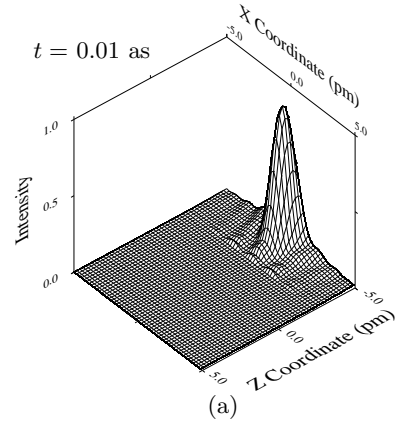


FIG. 3. 4 elements conventional Dirac field intensity. a:  $t = 0.01$  as, b:  $t = 0.02$  as, c:  $t = 0.03$  as, d:  $t = 0.04$  as.

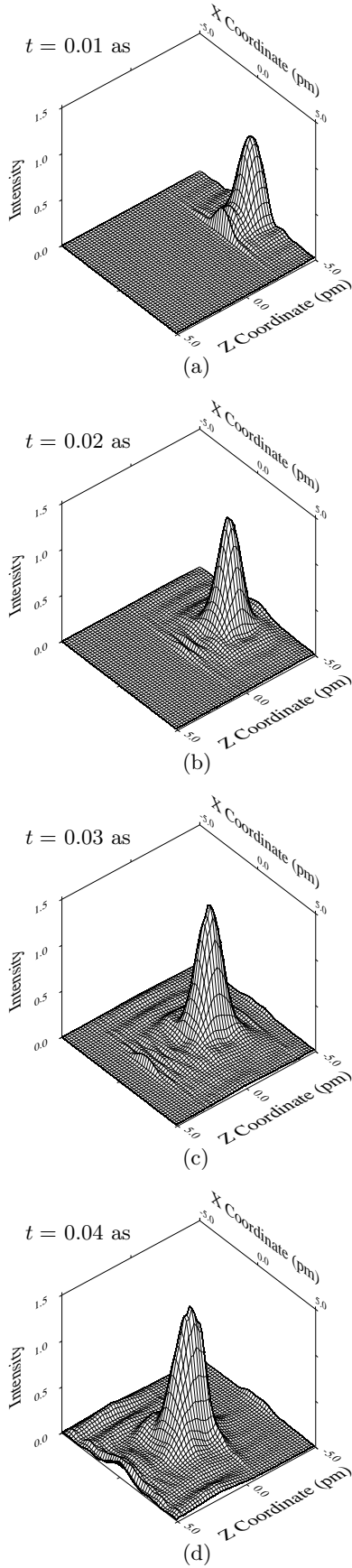


FIG. 4. 8 elements extended Dirac field intensity. a:  $t = 0.01$  as, b:  $t = 0.02$  as, c:  $t = 0.03$  as, d:  $t = 0.04$  as.

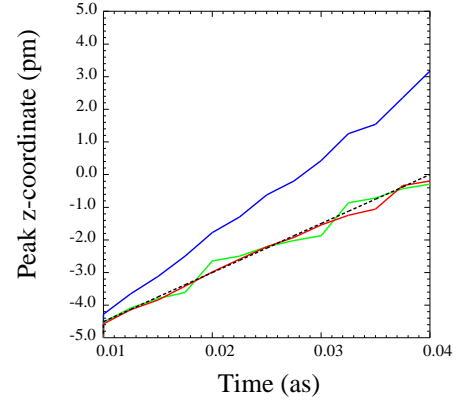


FIG. 5. Peak z-coordinate dependence on time.  $\beta = 0.5$ . blue: 2 elements (1-D like), green: 4 elements, red: 8 elements, broken black: theoretical value.

#### IV. SIMULATION FOR FORMATION PROCESS OF ATOMIC ORBITALS

In the electric central force potential  $\phi = Ze/4\pi\epsilon_0 r$  generated by an atomic nucleus with its atomic number of  $Z$ , the extended Dirac equations are given by

$$\begin{aligned} \left( i\partial_0 + \frac{e\phi}{\hbar c} + \delta^k \partial_k \right) \psi_A - \frac{mc}{\hbar} \psi_B &= 0, \\ \left( -i\partial_0 - \frac{e\phi}{\hbar c} + \delta^k \partial_k \right) \psi_B + \frac{mc}{\hbar} \psi_A &= 0, \end{aligned} \quad (36)$$

and

$$\begin{aligned} \left( i\partial_0 + \frac{e\phi}{\hbar c} \right) \psi_+ + \delta^k \partial_k \psi_- - \frac{mc}{\hbar} \psi_+ &= 0, \\ \left( i\partial_0 + \frac{e\phi}{\hbar c} \right) \psi_- + \delta^k \partial_k \psi_+ + \frac{mc}{\hbar} \psi_- &= 0. \end{aligned} \quad (37)$$

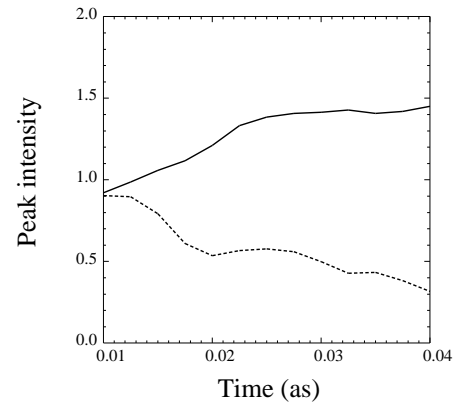


FIG. 6. Peak intensity dependence on time. solid line: 8 elements, broken line: 4 elements.

We calculated the extended Dirac field propagation by using the above method based on Eq. (37), where the velocity parameter  $\beta$  of the injected electron is 0.5. Figure 7 (a) and (b) show the log scale intensity on xz-plane at the early propagation time of 0.03 as and 0.035 as. We found that after  $t = 0.03$  as, a cone shape peak appears at the origin and rapidly grows up with increase of the propagation time, while the injected wave packet peak intensity decreases simultaneously. In this period, the cone shape wave function around the origin is proportional to  $\exp(-r/r_{init})$ , where  $r_{init}$  denotes the radius of the initial orbital. As shown in Fig. 7 (c),  $r_{init}$  is in invers proportion to atomic number  $Z$  and  $r_{init}$  is much smaller than analytical value of  $r_B/Z$  given by Schrödinger equation, where  $r_B$  is Bohr radius. Since Eq. (36) gives the following equations

$$\begin{cases} \left\{ \square - \frac{2ie\phi}{\hbar c} \partial_0 - \frac{e^2\phi^2}{\hbar^2 c^2} + \frac{m^2 c^2}{\hbar^2} + \frac{e}{\hbar c} (\delta^k \partial_k \phi) \right\} \psi_A = 0, \\ \left\{ \square - \frac{2ie\phi}{\hbar c} \partial_0 - \frac{e^2\phi^2}{\hbar^2 c^2} + \frac{m^2 c^2}{\hbar^2} - \frac{e}{\hbar c} (\delta^k \partial_k \phi) \right\} \psi_B = 0, \end{cases} \quad (38)$$

when we assume that the time dependent wave function is proportional to  $\exp(-r/r_{init} - i\omega t)$ , Eq. (38) creates the terms of  $r^{-n} \exp(-r/r_{init} - i\omega t)$  for  $(n = 0, 1, 2)$  and the term for  $n = 0$  gives

$$-\frac{\omega^2}{c^2} - \frac{1}{r_{init}^2} + \frac{m^2 c^2}{\hbar^2} = 0. \quad (39)$$

Therefore, if  $r_{init}$  is less than  $\hbar/mc \approx 0.39$  pm,  $\omega^2$  is negative and  $\omega$  is imaginary value, which means the absolute value of the wave function  $\exp(-r/r_{init} - i\omega t)$  exponentially increases with time and finally overflow of the peak intensity occurs. In order to avoid the overflow, we tried to set the limit of  $10^3$  for the absolute value of every element of the wave function in the spherical region of  $r < 0.5$  pm. Figure 8 shows the log scale intensity on xz-plane dependence on the propagation time, where the intensity limit exists around the origin and the side length  $L$  of the calculation cube is 20 pm. At  $t = 0.05$  as, a small cone shape orbital appears as same as Fig. 8, the radius of the orbital increases with time passing after 0.055 as. After  $t = 0.095$  as, the large intensity region of the wave function spreads to whole region of the calculation structure and the orbital shape is almost constant after  $t = 0.17$  as in the region of  $r > 3$  pm.

At the final moment of  $t = 0.2$  as, the wave function of the outer part of the orbital is assumed to be proportional to  $\exp(-r/r_{final})$ , where  $r_{final}$  is the radius of the final orbital. In Fig. 9, the solid line shows  $r_{final}$  dependence on the reciprocal of atomic number and the broken line shows the  $r_{final} = Z/r_B$ . Since it is known that 1s atomic orbitals are proportional to  $\exp(-Zr/r_B)$  [22], the calculation result could be right, because  $r_{final}$  almost coincides with the theoretical value given by Schrödinger equation.

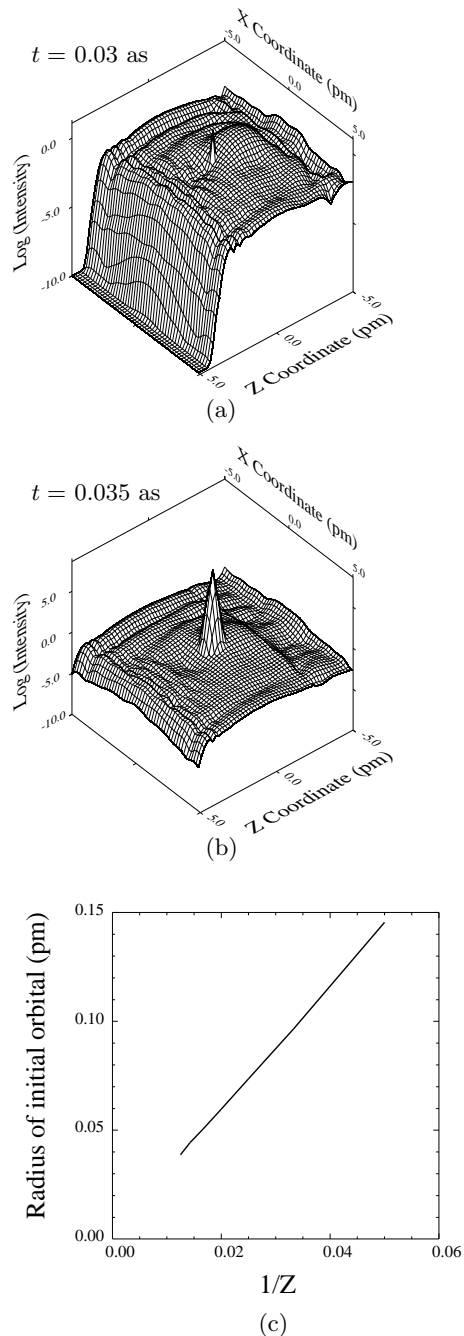
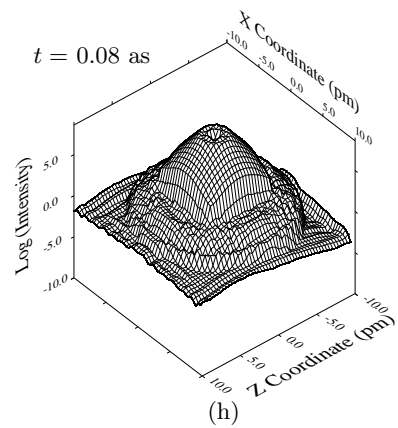
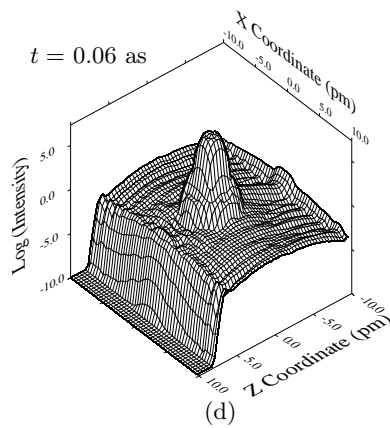
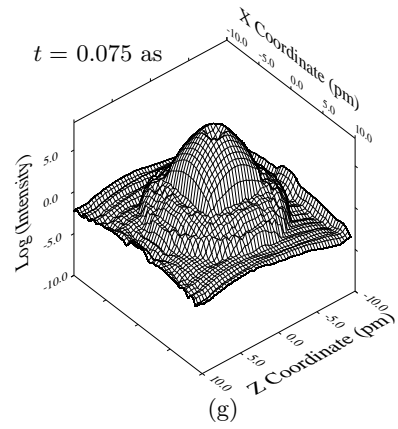
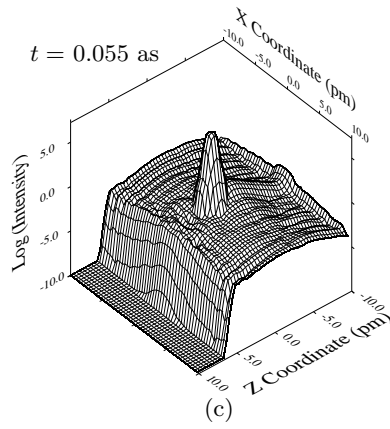
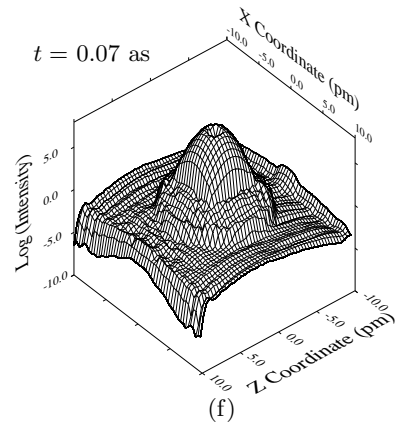
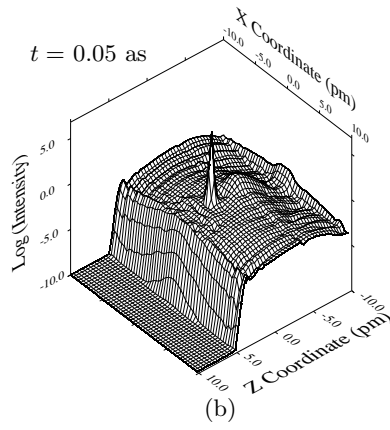
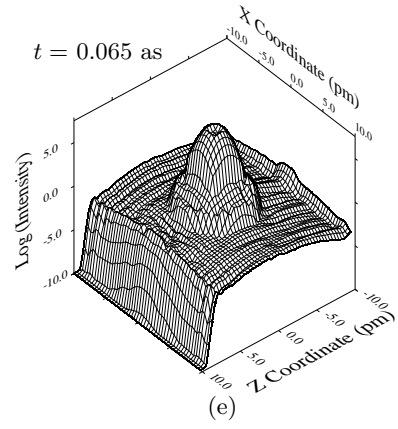
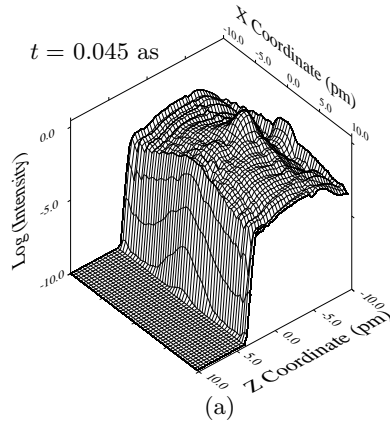


FIG. 7. Time dependence of Dirac field intensity in the potential of  $Ze/4\pi\epsilon_0 r$  with  $Z = 50$  for  $t = 0.03$  as (a) and  $t = 0.035$  as (b) and the initial orbital radius dependence on  $1/Z$  (c).



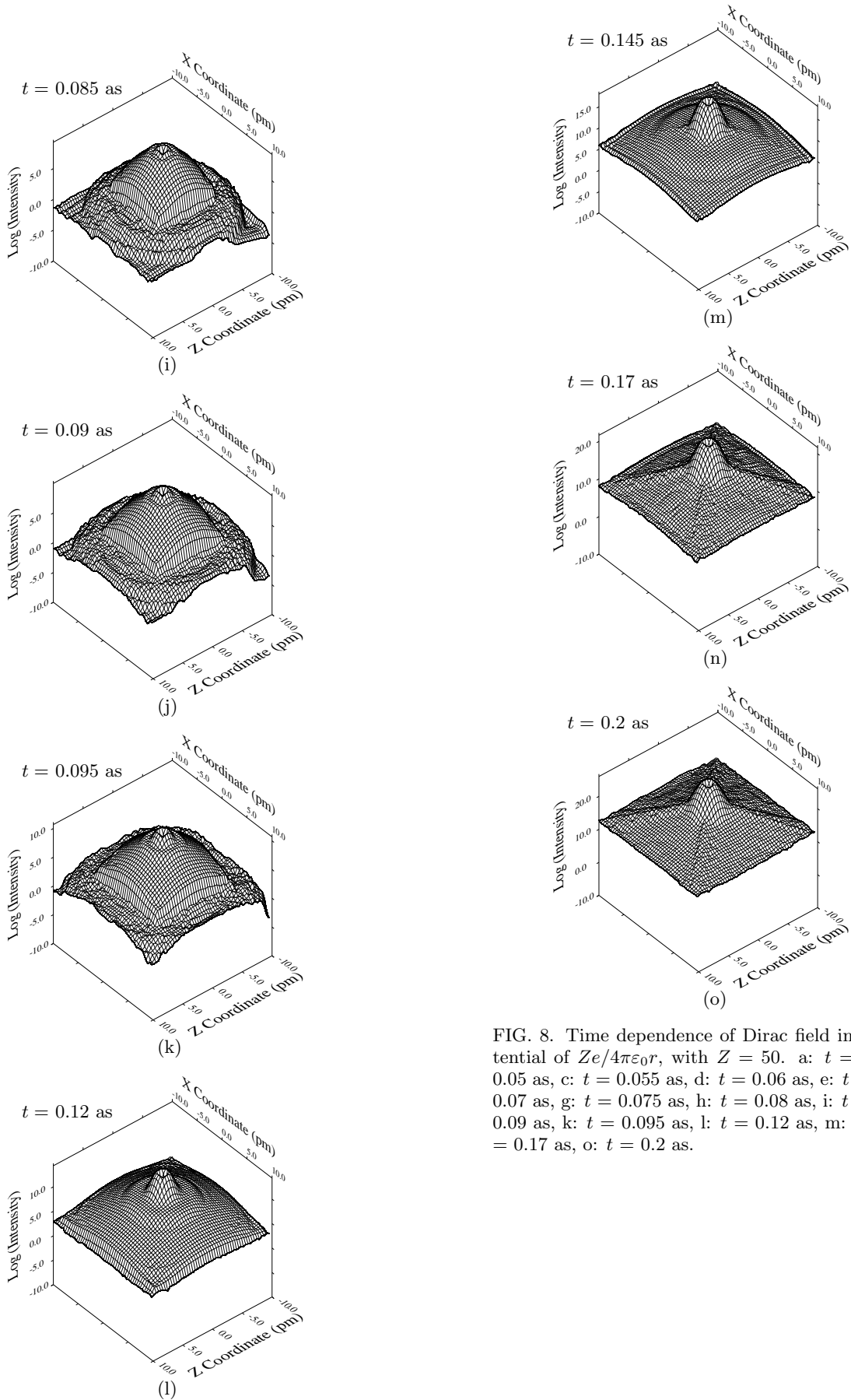


FIG. 8. Time dependence of Dirac field intensity in the potential of  $Ze/4\pi\epsilon_0 r$ , with  $Z = 50$ . a:  $t = 0.045$  as, b:  $t = 0.05$  as, c:  $t = 0.055$  as, d:  $t = 0.06$  as, e:  $t = 0.065$  as, f:  $t = 0.07$  as, g:  $t = 0.075$  as, h:  $t = 0.08$  as, i:  $t = 0.085$  as, j:  $t = 0.09$  as, k:  $t = 0.095$  as, l:  $t = 0.12$  as, m:  $t = 0.145$  as, n:  $t = 0.17$  as, o:  $t = 0.2$  as.



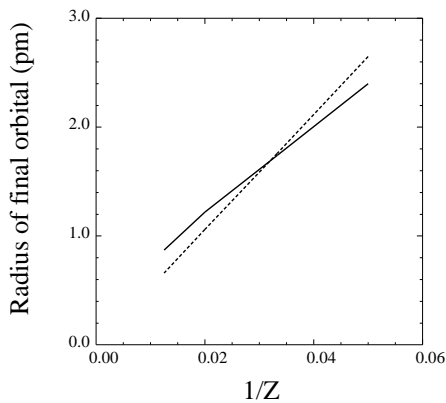


FIG. 9. Final orbital radius dependence on  $1/Z$ . Solid line: calculation value by FDTD method based on the extended Dirac equation, broken line:  $r_{final} = Z/r_B$  which is analytical solution by Schrödinger equation.

## V. CONCLUSION

Considering the charge creation-annihilation field, the extended Maxwell's and Dirac equations can be given by the same formula consisting of the dual 4-vector fields and the 8 by 8 spatially symmetric differential operator matrix. By 3D simulations using FDTD method, we found that the Dirac field wave packet with enough smaller velocity than light can be stably created without explicit consideration of Zitterbewegung, although it is difficult in 1D simulations. We succeeded to simulate the formation process of atomic orbitals based on the extended Dirac equation without any physical approximation for the first time. A small unstable orbital appears at first and rapidly grows and finally becomes to a large stable orbital with the same radius as Bohr radius divided by the atomic number given by Schrödinger equation. This result could be regarded as a proof of correctness of the charge creation-annihilation field model. It is expected that this method will be used for not only atomic physics but also particle physics and chemical reaction based on the spatial distribution of molecular orbitals [23].

- 
- [1] N. Nakanishi, *Progr. Theor. Phys.* **35**, 1111 (1966).
  - [2] N. Nakanishi, *Progr. Theor. Phys. Suppl.* **51**, 1 (1972).
  - [3] B. Lautrup, K. Danske Vidensk, *Selk. Mat.-fis. Medd.* **35**, no. 11 (1967).
  - [4] A. Taflove and S. C. Hagness, *Computational Electrodynamics: The Finite-Difference Time-Domain Method third edition* (Artech House, 1995).
  - [5] N. Simicevic, arXiv **physics.comp-ph**, 0812.1807v1 (2008).
  - [6] N. Simicevic, arXiv **quant-ph**, 0901.3765v1 (2009).
  - [7] P. A. M. Dirac, *The principles of quantum mechanics fourth edition* (Oxford, 1958).
  - [8] M. E. Peskin and D. V. Schroeder, *An Introduction to Quantum Field Theory* (Westview, 1995).
  - [9] F. Mandl and G. Shaw, *Quantum Field Theory 2nd ed.* (Wiley, 2010).
  - [10] J. J. Sakurai, *Modern quantum mechanics second edition* (Addison-Wesley, 2011).
  - [11] H. Mutoh, *J. Institute of Image Information and Television Engineers* **67**, J89 (2013), [https://www.jstage.jst.go.jp/article/itej/67/3/67\\_J89/\\_pdf](https://www.jstage.jst.go.jp/article/itej/67/3/67_J89/_pdf).
  - [12] H. Mutoh, *Proc. 2013 Int. Image Sensor Workshop* **7.01**, 189 (2013).
  - [13] H. Mutoh, *IEEE Trans. Electron Devices* **63**, 49 (2016).
  - [14] H. Mutoh, *Proc. Int. Conf. on Simulation of Semiconductor Process and Devices 2014*, 225 (2014).
  - [15] H. Mutoh, *Proc. 2018 Progress in Electromagnetics Research Symposium*, 2537 (2018).
  - [16] H. Mutoh, *Proc. 2019 Progress in Electromagnetics Research Symposium*, 1749 (2019).
  - [17] S. M. Sze, *Physics of Semiconductor Devices* (Wiley, New York, 1981).
  - [18] A. S. Grove, *Physics and Technology of Semiconductor Devices* (Wiley, New York, 1967).
  - [19] S. Selberherr, *Analysis and Simulation of Semiconductor Devices* (Springer, Wien, 1984).
  - [20] E. Schrödinger, *Zur Quantendynamik des Elektrons*, 63 (1931).
  - [21] J. J. Sakurai, *Advanced quantum mechanics* (Addison-Wesley, 1967).
  - [22] L. I. Schiff, *Quantum Mechanics third edition* (McGraw-Hill, 1970).
  - [23] K. Ohno, H. Mutoh, and Y. Harada, *Journal of the American Chemical Society* **105** (14), 4555 (1983).